N-35-CR
170243
P-29

NASA NAS7-1002
NASA CR-
PSI-1038/TR-876

MULTICOLOR PYROMETER FOR MATERIALS PROCESSING IN SPACE

PHASE II

Quarterly Report No. 5

Michael Frish, Jonathan Frank, Henry Beerman
Physical Sciences Inc.
Research Park, P.O. Box 3100
Andover, MA 01810

For the Period 1 June - 31 August 1988

November 1988

Prepared for:

NASA - Jet Propulsion Laboratory
4800 Oak Grove Drive
Pasadena, CA 91109

(NASA-CR-183358) MULTICOLOR PYROMETER FOR MATERIALS PROCESSING IN SPACE, PHASE 2 Quarterly Report No. 5, 1 Jun. - 31 Aug. 1988 (Physical Sciences) 29 p CSCL 14B

N89-14406

Unclas
G3/35 0170243

CONTENTS

FIGURES

1. INTRODUCTION

This report documents the work performed by Physical Sciences Inc. (PSI) under contract to NASA JPL, during the fifth quarter of a two-year SBIR Phase II program. The program goals are to design, construct and program a prototype passive imaging pyrometer capable of measuring, as accurately as possible, the temperature distribution across the surface of a moving object suspended in space. The approach is to utilize an optical system that operates at short wavelengths compared to the peak of the blackbody spectrum for the temperature range of interest, thus minimizing errors associated with a lack of knowledge about the heated sample's emissivity. To cover a broad range of temperatures, several wavelengths are required. The preferred wavelength decreases as the temperature increases.

Previously,[1] we performed a survey of available imaging technologies and selected the Sierra Scientific Model 4032 CCD camera as the sensor to be used by our pyrometer. An analysis of the system's temperature measurement capability based on this camera's responsivity was performed and found to be satisfactory. Subsequently, the camera was purchased and coupled to a Compaq 286 computer through a Data Translation Model 2851 frame-grabber. A unique interface between camera and computer was designed and assembled allowing the computer to electronically control the exposure time of each frame.[2] The overall system noise was measured as a function of integration time for use in optimizing the pyrometer's operation.[3]

We had also reported previously several conceptual designs of the optical system which will image the sample onto the CCD detector.[2] The designs were intended to maximize use of the detector's spatial resolution by projecting images at all of the desired wavelengths simultaneously, thereby eliminating the need for moving parts. However, as reported in the last quarter,[4] each early optical design posed insurmountable difficulties when attempts were made to construct working breadboard models. We are pleased to report here that a viable optical design which projects six different wavelength images has now been completed, and a working three-color version of this design has been assembled in breadboard form. An engineering design of the complete six-color system has been completed and machining of components is underway. In addition, algorithms have been developed and programmed for: rapidly calibrating the system, automatically selecting which one of the multiple images is appropriate for calculating temperature, rapidly determining the temperature distribution and average temperature of the object from that image, and displaying a false-color temperature map of the object. The system has been assembled so that this temperature information can be easily used in a feedback loop to control the temperature of the object.

Details of the optical system, along with some of the engineering drawings, are provided in Section 2 below. Section 3 discusses final selection of the six colors chosen for use in the pyrometer, and the data acquisition and analysis algorithms are described in Section 4.

2. OPTICAL SYSTEM

2.1 Description

The optical system employs the color separation scheme illustrated schematically in Figure 1 to project six different-colored images simultaneously onto the photosensitive surface of our camera's 6 mm x 4.5 mm CCD array. For convenience, only three colors are shown in the drawing. This system was designed to observe objects having diameters of about 2 mm moving within a spherical volume of about 1 cm diameter. Radiation emitted by the heated sample is collected by a 360 mm focal length objective lens. The sample is located nearly within the focal plane of the lens, thereby projecting a nearly-collimated beam of light into the color separator. (The half-angle divergence of the collimated beam is $\tan^{-1}(s/2f)$ where $s = 1$ cm is the linear dimension of the area viewed by the pyrometer, and $f = 360$ mm is the focal length of the objective lens.) This beam is separated into color ranges by a series of dichroic beamsplitters. The first beamsplitter ideally reflects all radiation at wavelengths greater than λ_1 while transmitting all shorter wavelengths. The second beamsplitter similarly reflects all radiation at wavelengths longer than λ_2 (of which there is ideally none longer than λ_1) and transmits the rest, which is reflected by the third mirror. The three reflected beams are transmitted through interference filters that select the desired narrow bands

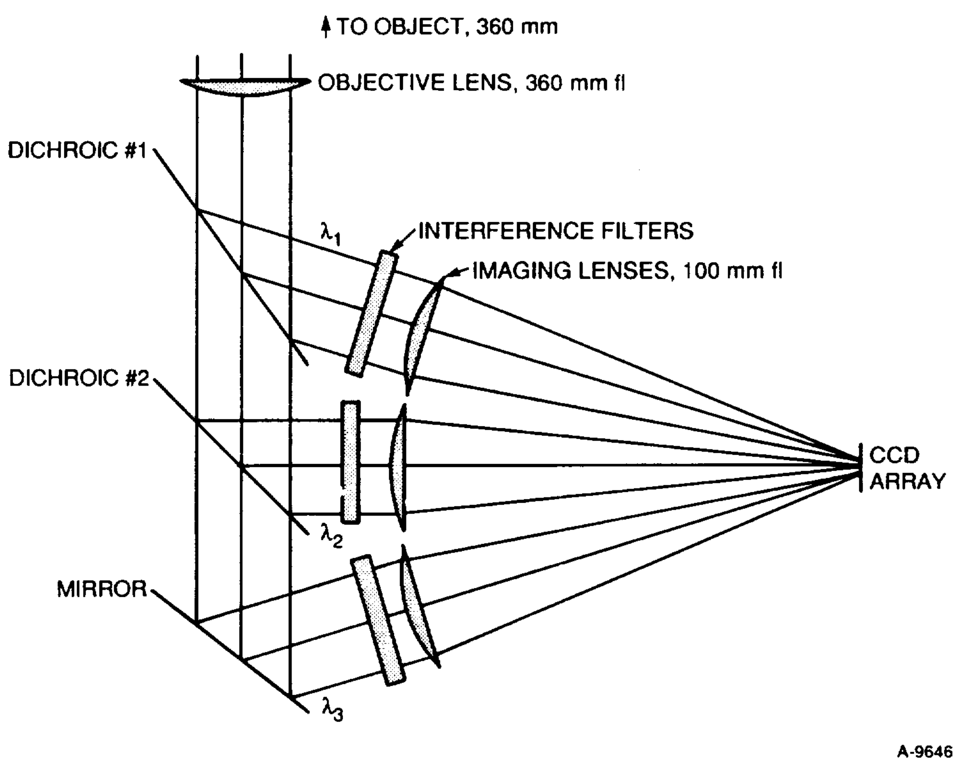

Figure 1. Schematic illustration of three-color separator.

of wavelengths from the relatively broad bands reflected by the beamsplitters, and thence through 100 mm focal length imaging lenses that image the sample onto the CCD array located at the focal plane of the lenses. The overall system magnification of 0.28 is determined by the ratio of the focal lengths of the objective lens to the imaging lenses.

To provide all six images, a fourth dichroic beamsplitter is inserted ahead of the three shown. It reflects a band of wavelengths upwards to a second row of beamsplitters. The reflections from this second layer are projected similarly onto the CCD as illustrated by the side view of Figure 2. The six optical paths are aligned so that the centers of the images are positioned on the CCD as illustrated in Figure 3. Each center is 1.5 mm from its neighbors, meaning that objects 1.5/0.28 = 5.3 mm in diameter can be observed without the images overlapping each other. Since the image centers are also at least 1.5 mm from the edge of the detector, each image is a projection of the full 1 cm field of view.

The optical collection efficiency of the system is limited by the 25 mm diameter imaging lenses to about F/14. To reduce optical aberrations, it is preferable to place a stop at the objective lens with a diameter no greater than 20 mm, limiting the speed to F/18. When operating at this speed there is no vignetting of objects moving within the field of view.

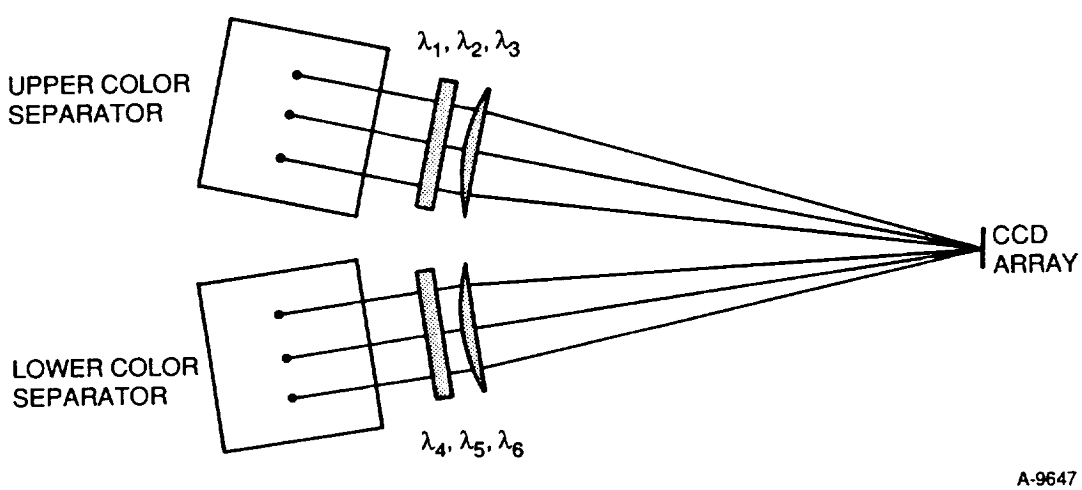

Figure 2. Side view of six-color projection system.

2.2 Engineering Design

As mentioned above, a three-color version of this optical design has been assembled in breadboard fashion and shown to work well, as long as the wavelengths are carefully selected to avoid incompatibilities among the various components, as discussed in Section 3 below. Furthermore, an engineering design for a structurally sound six-color system has been completed and is currently being machined. Drawings of the critical components and their layout comprise Figures 4 through 12. They are described in the following.

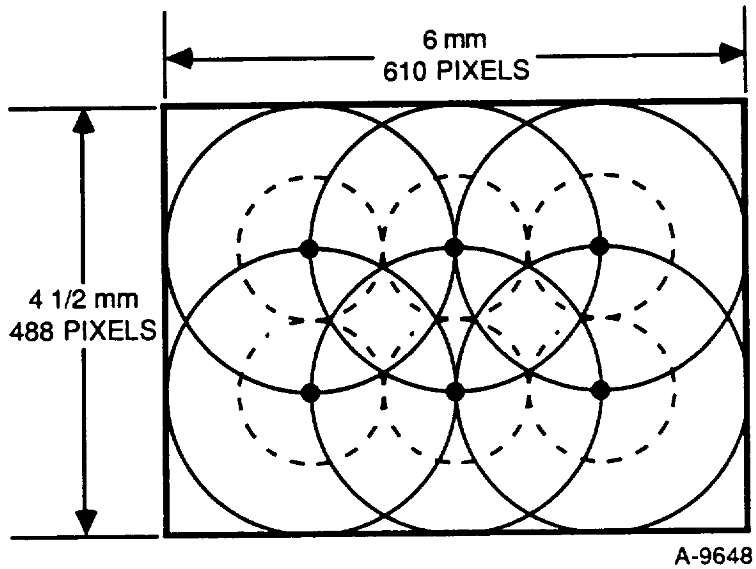

Figure 3. Illustration of areas covered on the CCD array by the six images. Note that objects smaller than 5.3 mm in diameter (dashed circles) do not have overlapping images.

Each of the two three-color beam separators is mounted on a platform, one of which is shown in Figure 4. The drawing is oriented so that the objective lens holder (shown in Figure 5) is positioned at the top of the L-shaped configuration, and the CCD camera is supported by a bracket (Figure 6) located at the right edge. Progressing from the objective lens, the platform holds a triangular mount (detailed in Figure 7) for the first beamsplitter, which separates the short wavelengths from the long and directs them upwards to the second color separator. Beyond this mount three holes are drilled in the baseplate at angles appropriate for attaching the three dichroic beamsplitters which comprise the long-wavelength color separator. Each of these 5 cm x 5 cm beamsplitters will be attached to a 2.54 cm x 2.54 cm adjustable mirror mount (supplied by the Newport Corporation) by means of the small holders illustrated in Figure 8. The centers of the three color-separated beams then follow the dashed lines and pass through a bracket (detailed in Figure 9) that holds a narrow band interference filter and imaging lens for each wavelength. The filter and lens are attached to each other by the housing illustrated in Figure 10, which in turn screws into the bracket to facilitate fine focusing of the image. Finally, the three images are incident on the CCD at the camera mounting bracket.

Figure 11 is a scale drawing of the layout of the optical components in one color separator. The locations and orientations of the three mirror mounts enable the center beam to be directed onto the CCD array at normal

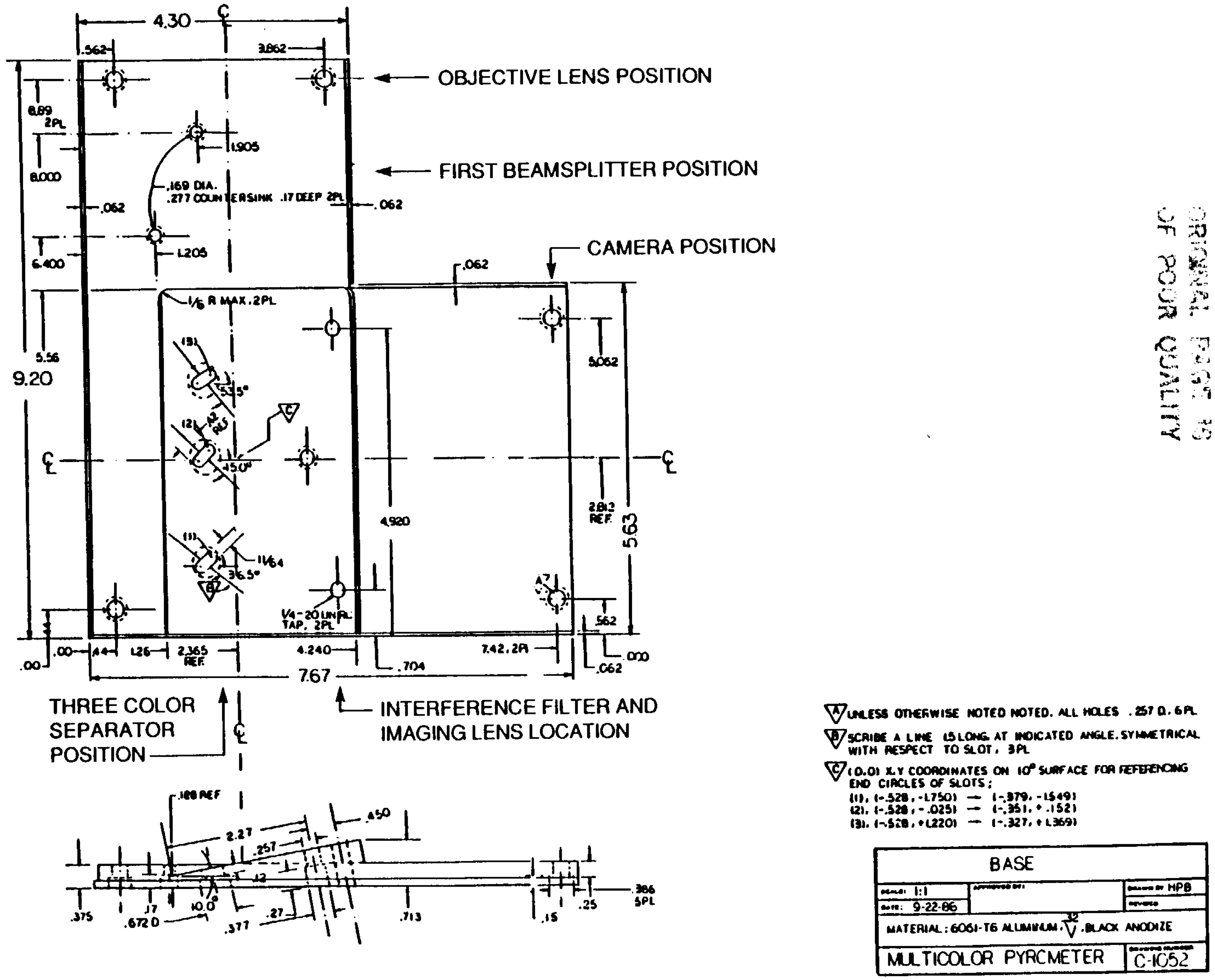

Figure 4. Base platform.

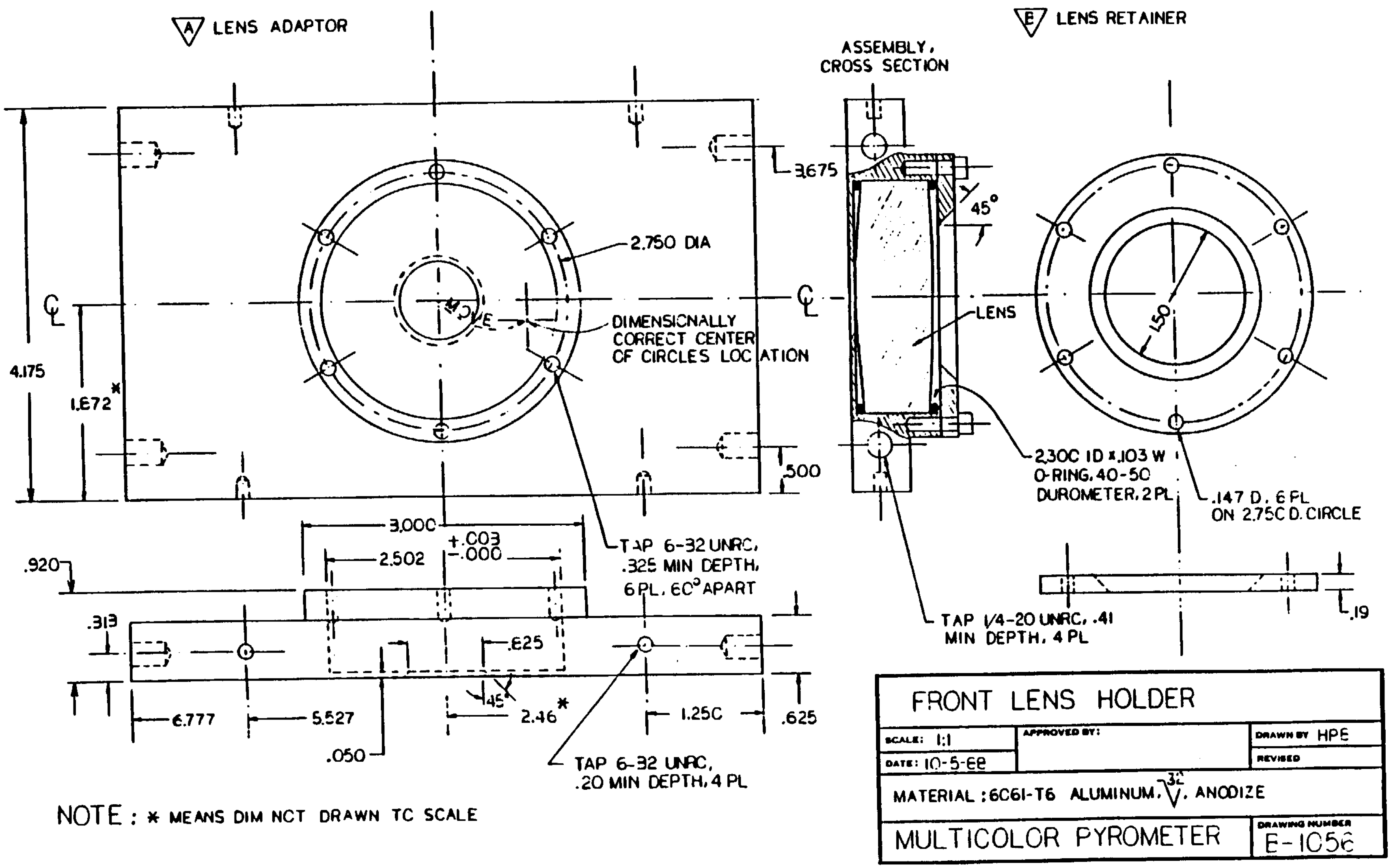

Figure 5. Objective lens mount.

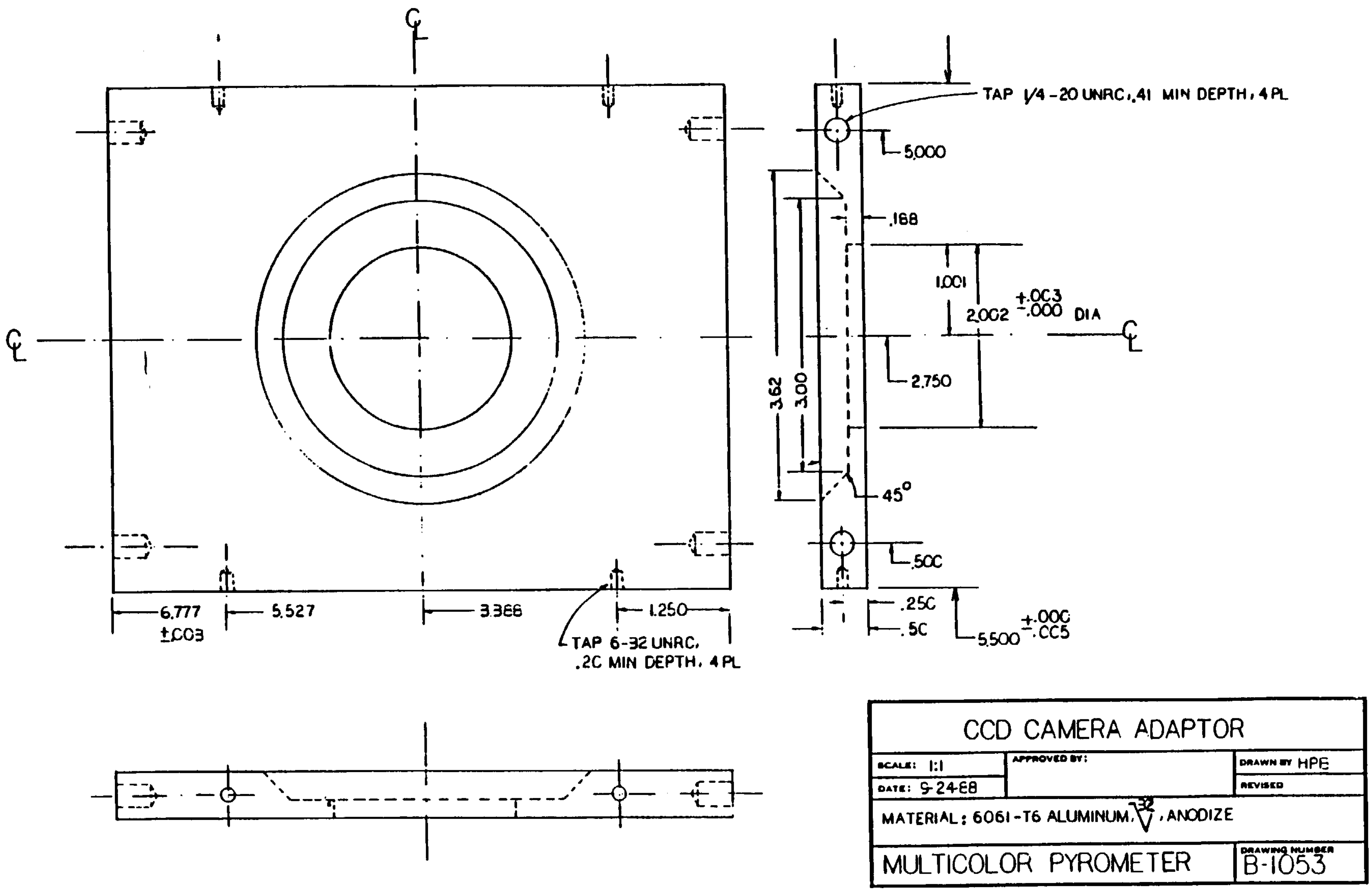

Figure 6. Camera mounting bracket.

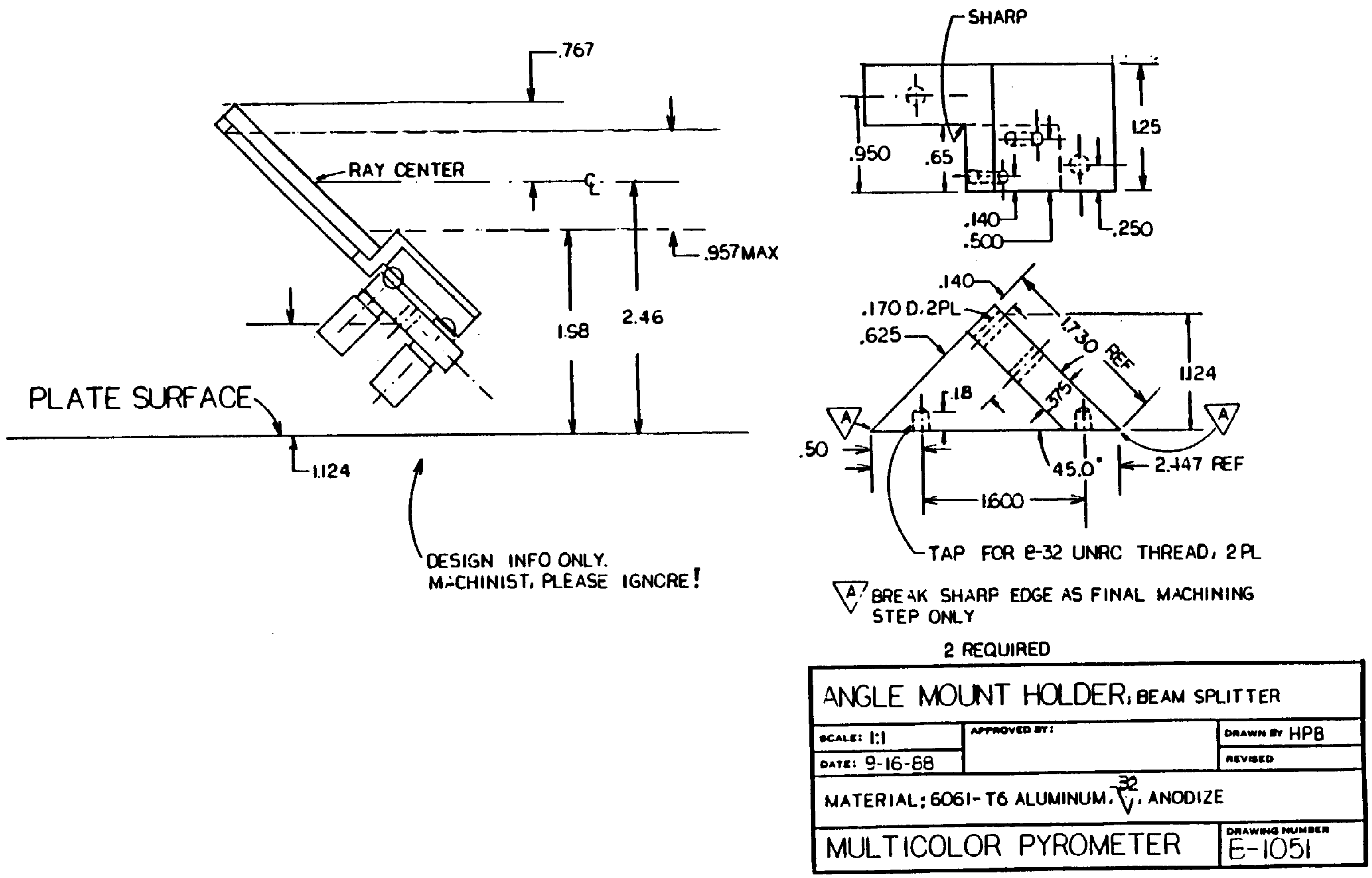

Figure 7. Beamsplitter mount.

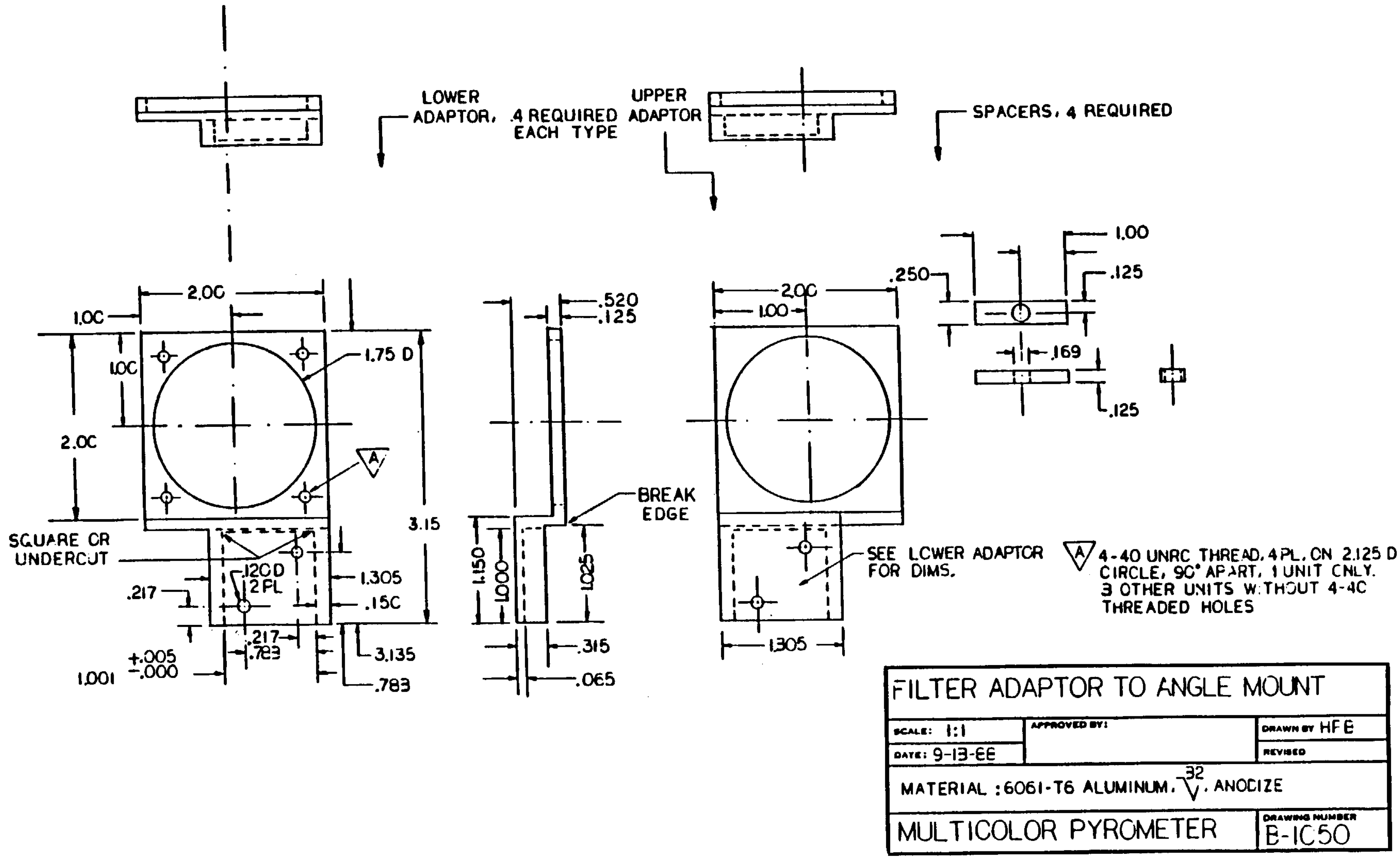

Figure 8. Dichroic mirror holders.

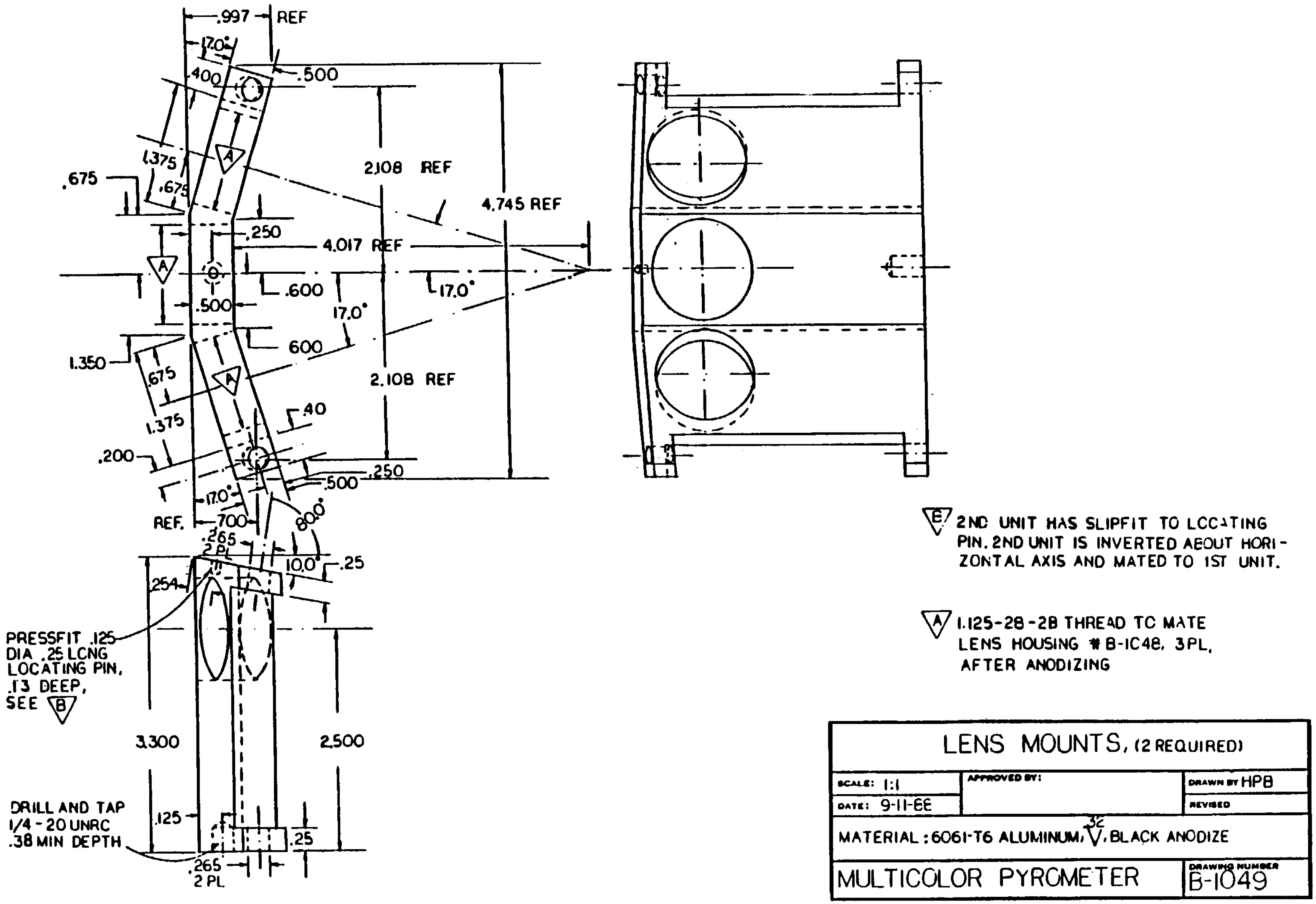

Figure 9. Lens and filter mounting bracket.

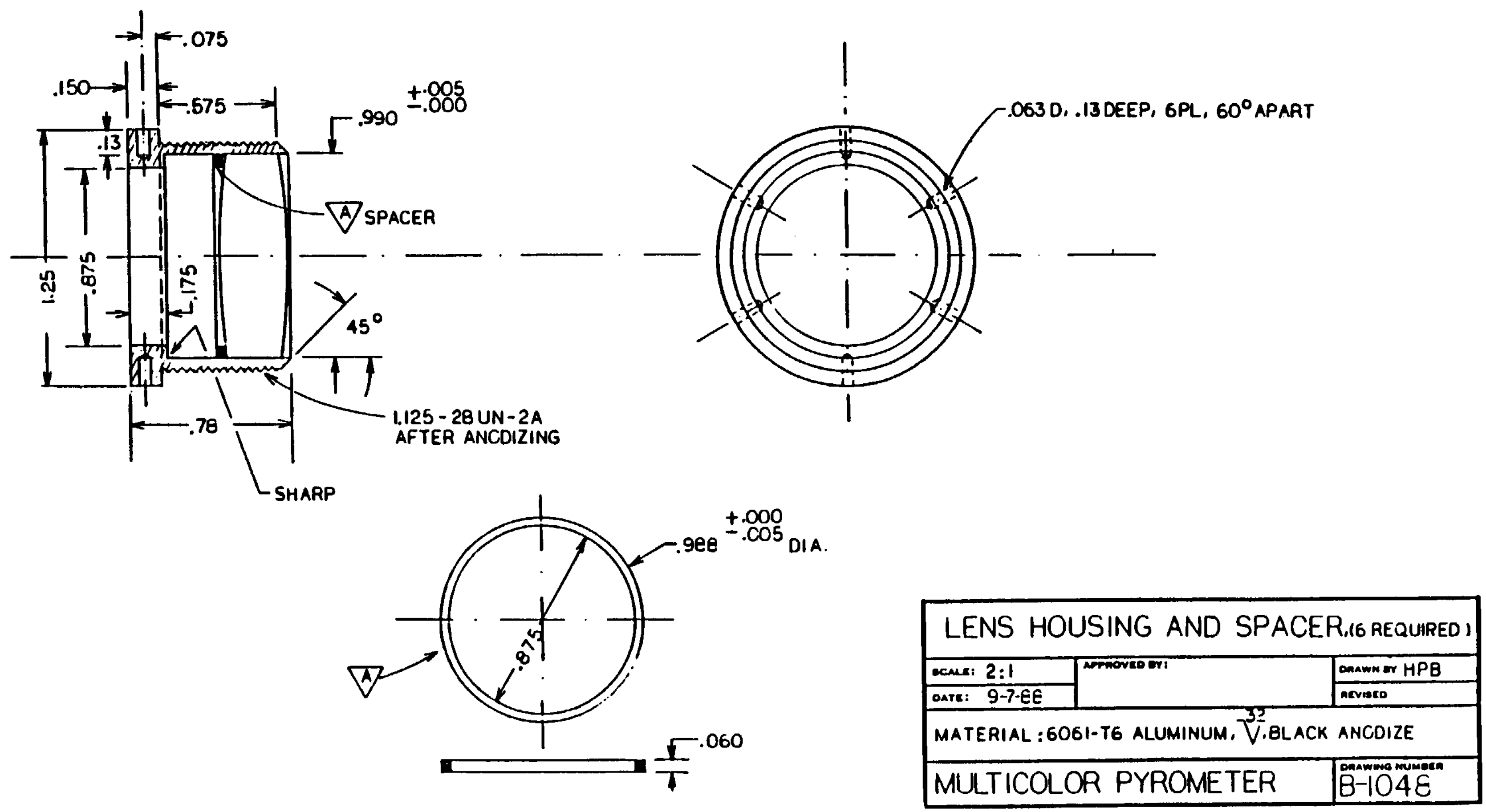

Figure 10. Lens and filter housing.

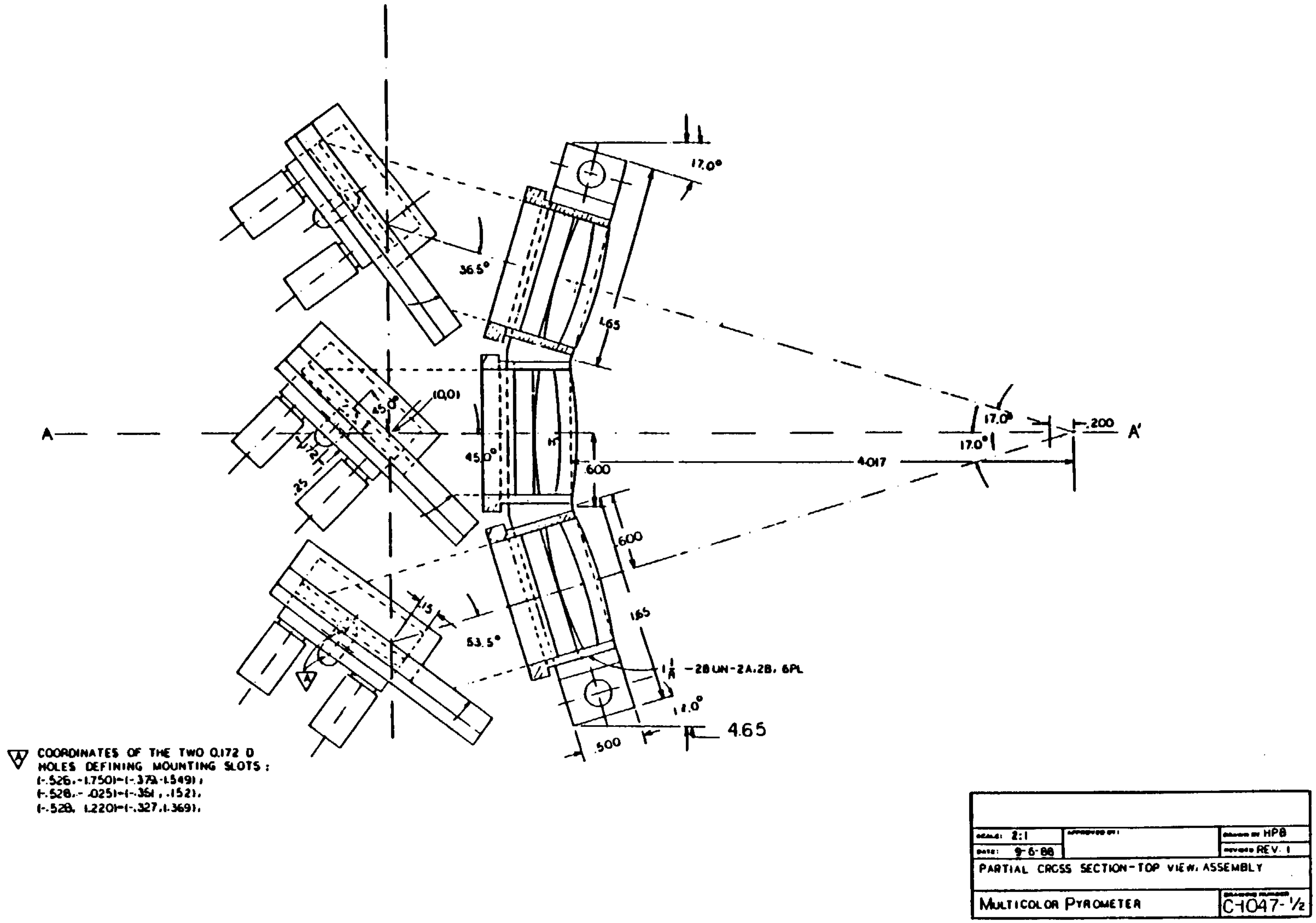

Figure 11. Layout of three-color separator components.

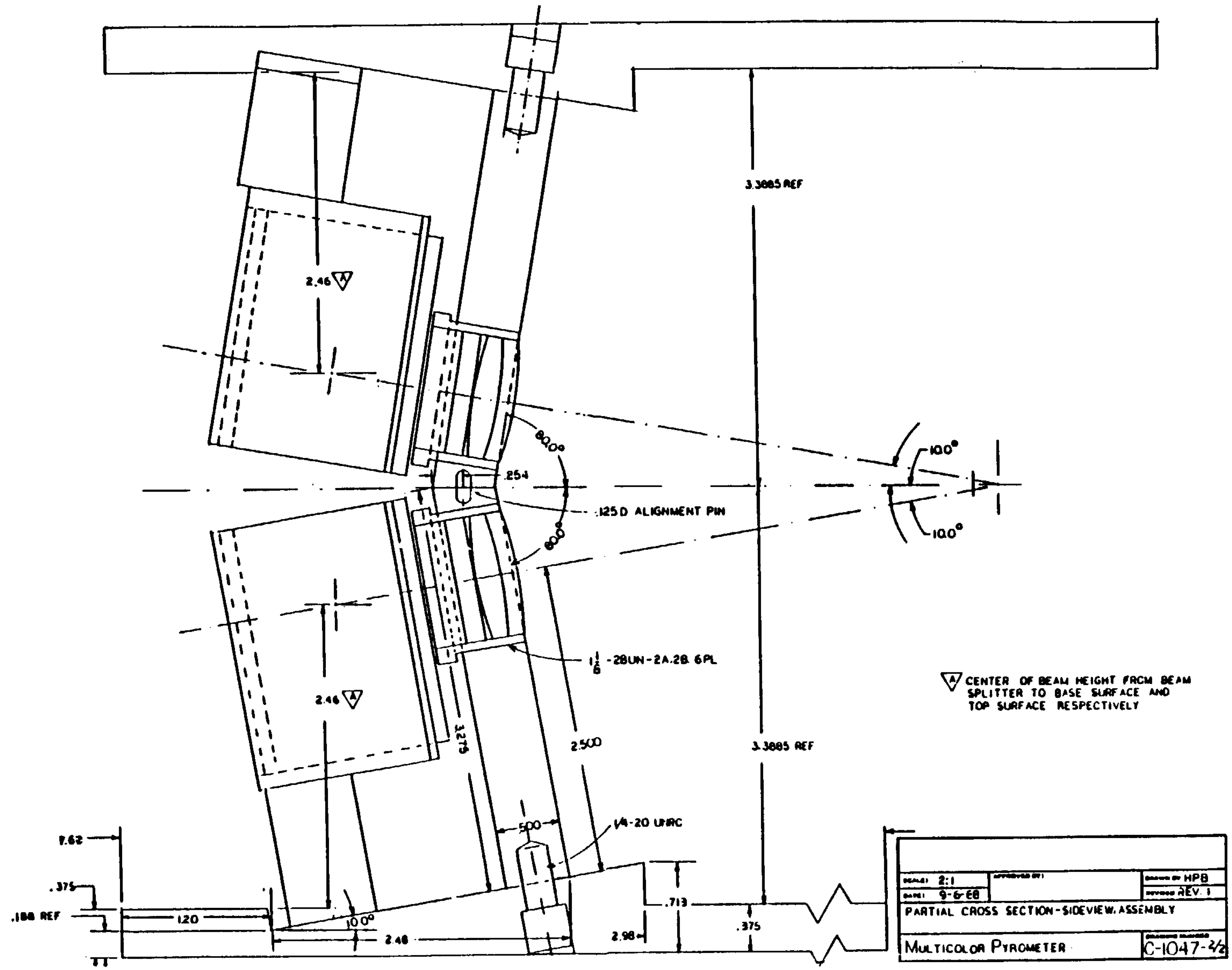

Figure 12. Side view showing configuration of dual color separators on mounting platforms.

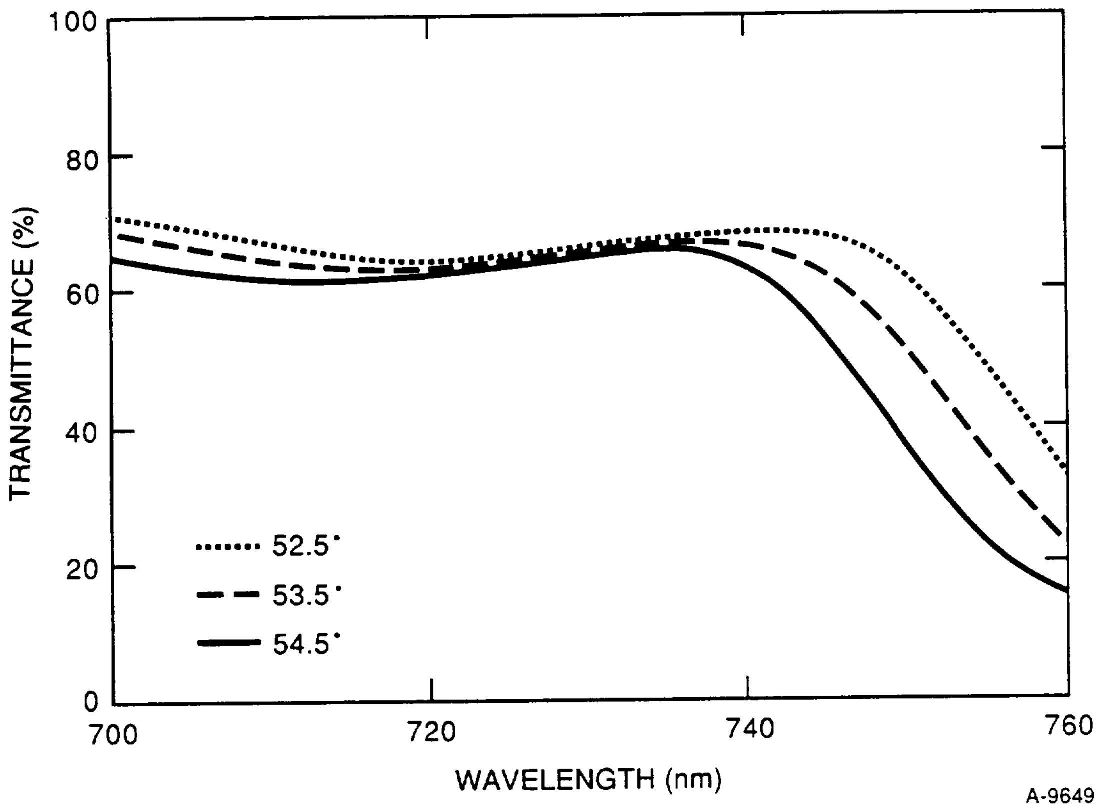

Figure 13. Transmission curve of Corion Model LS900 dichroic filter at three slightly different angles of incidence.

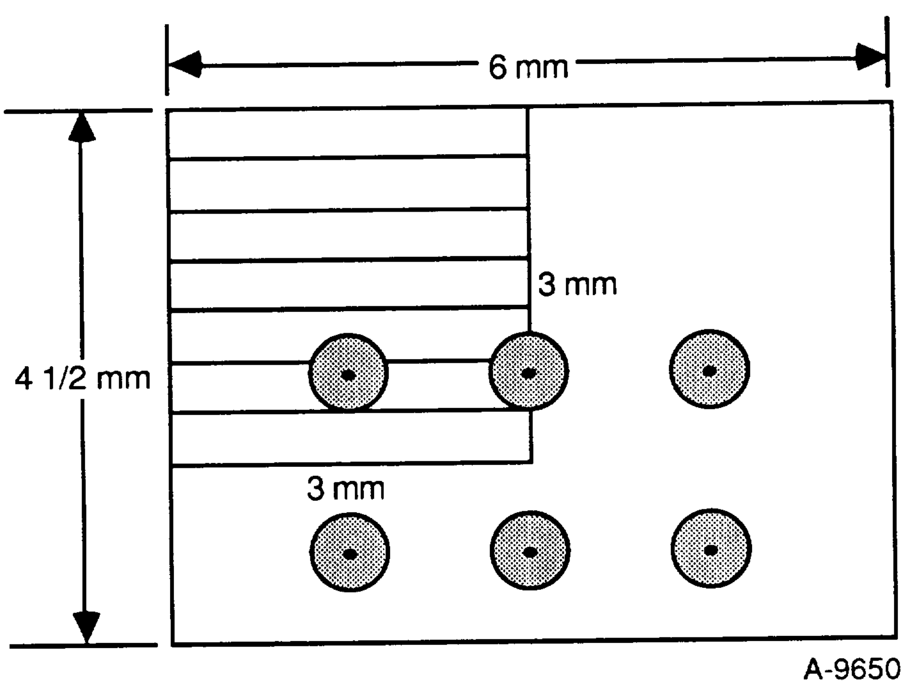

Figure 14. Image location procedure.

incidence and each of the two outer beams at an angle of 17 degrees, this being the minimum angle achievable when employing 2.54 cm diameter imaging lenses. The CCD array is located just ahead of the confluence of the three dashed lines which indicate the centerlines of the three beams. From the plan view of the mounting platform (Figure 4), it is seen that the beamsplitters and lens mounting bracket are oriented at a 10 deg angle relative to the vertical. The upper color separator is mounted similarly, so that the two sets of images are vertically separated by the desired distance (~1.5 mm) when projected onto the CCD array. Figure 12 is a plan view showing the mounting of the upper and lower color separators and the optical paths to the camera.

3. WAVELENGTH SELECTION

The algorithm used to select the six wavelengths was described in a previous report.[4] Briefly, colors are selected which provide the maximum measurement precision over the desired temperature range for a given optical configuration and exposure time. Using the optical design described in the previous section, an integration time of 1/60 s (standard video rate), a maximum temperature of 2500 K and a minimum temperature as small as possible for the optical system but no lower than 500 K, the colors indicated in Table 1 were found to be optimum for a material having an emissivity of about 0.5. (The effects of changing the emissivity were also discussed in the previous report.) The range of temperatures spanned by each color while providing a measurement precision of 0.2 percent are tabulated along with the ranges measurable regardless of precision.

Table 1. Pyrometer Wavelengths and Temperature Ranges

Wavelength (nm)	High Temperature (K)	Low Temperature at 0.2% Precision	Absolute Minimum Temperature
930	1302	1119	888
750	1506	1298	1050
590	1728	1505	1244
480	1971	1726	1445
420	2249	1970	1650
370	2562	2243	1878

Off-the-shelf optical components were purchased to assemble the breadboard system at these wavelengths. However, because of some unexpected characteristics of the dichroic beamsplitters, slight adjustments of the wavelengths were required to assure uniform transmission of the collimated beam over its entire diameter. The reason for these adjustments is as follows: It had been assumed for design purposes that the dichroic filters had sharp transition wavelengths, i.e., below the cutoff wavelength the transmission is a constant (ideally unity) independent of wavelength, and above the cutoff the transmission is a different constant (ideally zero). Unfortunately, the ideal is not met in reality. Figure 13 shows typical curves of transmittance versus wavelength at three slightly different angles of incidence for the dichroic beamsplitter intended to transmit wavelengths shorter than 800 nm and reflect all others. Fairly large variations in the transmittance as a function of wavelength are obvious. Furthermore, the transition from transmissive to reflective appears to begin at about 740 nm and is spread out over a broad band of wavelengths. This occurs because the manufacturer's specification of the cutoff wavelength was for an incident angle of 45 deg, and the curves shown were obtained at the actual incidence angles around 52.5 deg. Though the difference between the specified and actual angle of incidence is small, it results in a surprisingly large change in the beamsplitter's characteristics.

The rapid change in transmittance with varying angles of incidence is most severe near the cutoff wavelength, which has shifted to about 740 nm and is now below the pyrometer wavelength of 750 nm selected to measure temperatures between 1300 and 1500 K. This is especially troublesome since the finite (1 cm) field of view imaged by the pyrometer causes the collimated beam transmitted through the wavelength separator to actually diverge with a half angle of $\tan^{-1}(5/360) = 0.8$ deg. As a result, different parts of the beam, when transmitted through this beamsplitter, experience dramatically different transmittance at some wavelengths, potentially yielding a very non-uniform image that would make for a poor pyrometer indeed. In particular, the transmittance at 750 nm shows a 30 percent change as the incident angle varies between 51.5 and 53.5 deg. This combination of wavelength, angle of incidence and beamsplitter is clearly unusable. The problem was alleviated by adjusting the wavelength to one where the transmission was nearly uniform over the bandpass of the filter, which in this case occurs at a central wavelength of about 735 nm, resulting in an insignificant change in the usable temperature range.

4. DATA ACQUISITION AND PROCESSING ALGORITHMS

The temperature measurement and display process comprises the steps of: 1) acquiring a frame of data; 2) selecting the appropriate one of the six available images for analysis; 3) subtracting the dark signal from that image; and 4) converting the radiance data in the image to temperature values. The last step assumes, of course, that the system has been precalibrated so that the correspondence between measured radiance and temperature is known. The procedures for acquiring frames have been discussed in detail in the past. Here we describe the data reduction procedures.

4.1 Background Frame

As discussed in our second quarterly report, each pixel in the CCD camera has a unique but constant dark current which produces a dark signal that is a function of the integration time. To obtain accurate temperature measurements, this dark signal is subtracted from each frame of data. The average background signal is obtained simply by blocking the pyrometer's entrance aperture, adjusting the integration time to the desired value, and collecting a sequence of 100 frames. Average values of the gray level at each pixel are stored in a 512 x 512 byte block of computer memory and called up as required for background subtraction.

A portion of this background frame is subtracted from each data frame. The frame subtraction procedure is currently rather slow, requiring about 1s to subtract an entire frame since the data must be transferred from the frame grabber, across the computer bus, and back to the frame grabber. This is necessary because the frame grabber has sufficient storage capacity for only two frames, and both of these buffers are needed for the data acquisition process, as described in a previous report. We currently minimize the subtraction time by operating only on that region of the frame which contains the relevant image, as described below, thus reducing the background subtraction time by at least a factor of six compared to full frame subtraction. In the near future we intend to upgrade the system with a new frame grabber that has sufficient storage capacity to include the background frame, and is able to perform the subtraction without transferring data to the computer's main memory. This will enable background subtraction as the data frame is collected.

4.2 Image Selection

As described above, the pyrometer projects six non-overlapping images onto the CCD array simultaneously, but only one image provides data suitable for reduction to temperature. All of the other images are either bright enough to saturate the frame grabber, or dim enough to be undetectable. Selection of the correct image is therefore accomplished by scanning selected portions of a data frame to locate pixels which have non-zero but unsaturated gray levels.

If the objects observed by the pyrometer were stationary and of nearly uniform temperature, then this task would require only a quick measurement of the gray levels at the known center points of each image. However, as mentioned previously, the objects are expected to be about 2 mm in diameter and are allowed to move within a 1 cm diameter volume. Thus, as illustrated in Figure 3, each image moves within a 3 mm diameter area on the CCD array.

Though the six images move about, their relative positions remain constant. Therefore, to locate the centers of the images it is necessary to scan the data frame to find the center of only one image - all of the other centers are then a known distance away. To find the first center, the intensities are measured of the pixels lying along several lines cut through the 3 mm x 3 mm area in which the longest wavelength image can be found, as illustrated in Figure 14. Assuming the object is spherical and at least 2 mm in diameter, then only six evenly spaced horizontal lines need be scanned to locate it. To find the center of the object, the pixel values outside of it are assumed to be below some threshold. The algorithm, shown in flowchart form in Figure 15, first determines which of the six horizontal lines contains pixels having gray values above the threshold, and then finds the horizontal positions of the transitions from below to above threshold and vice versa. The abscissa of the image center is the midpoint between these two edges. The ordinate is found by performing the same operation along a vertical line that passes through the abscissa.

This procedure is performed on the image used to measure the lowest temperatures. If an image is found, it will either provide usable data or will be saturated. If it is saturated, then the center of the image corresponding to the next longest wavelength, located 1.5 mm away from the first image, is checked for saturation. This procedure is repeated until an unsaturated image is found.

4.3 Calibration

Calibration of the pyrometer is performed by placing a calibration source (such as a blackbody) of known temperature and emissivity in the focal plane, measuring the gray level of the image at the appropriate wavelength, and calculating the temperature corresponding to other gray levels at that wavelength from the Planck equation. Details of the algorithm are shown in the flowchart of Figure 16. The center of the image is located using the algorithm discussed above. A 0.6 mm x 0.6 mm square is then circumscribed around the image (corresponding to 2 mm x 2 mm in the object plane) and the background subtracted from the region enclosed by the square. A histogram of gray values for the pixels within the square is then calculated and the peak value of this histogram recorded. The procedure is repeated 100 times, and the average value of the histogram peak is calculated. This average is then used to calculate the calibration constant at that wavelength. Using this calibration constant, a lookup table is calculated which relates each of the 256 available gray levels within the image to a corresponding temperature. The lookup table is stored for use during data acquisition.

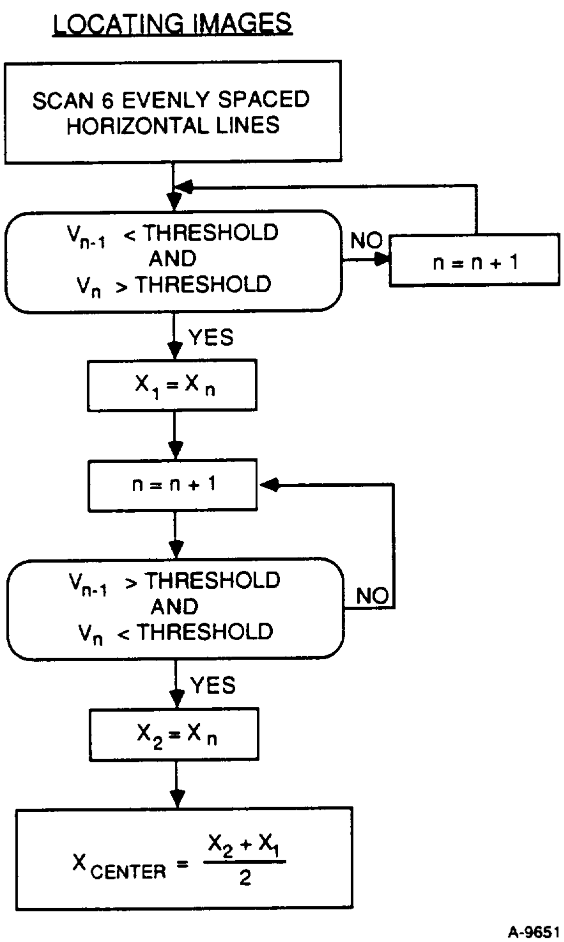

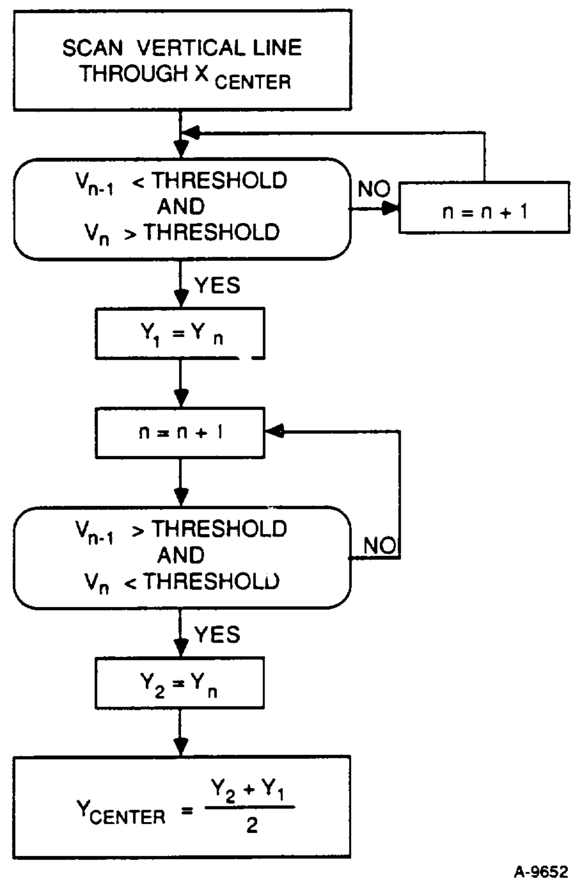

Figure 15a. Flowchart of algorithm for finding abscissa of image center.

Figure 15b. Procedure for finding ordinate of image center.

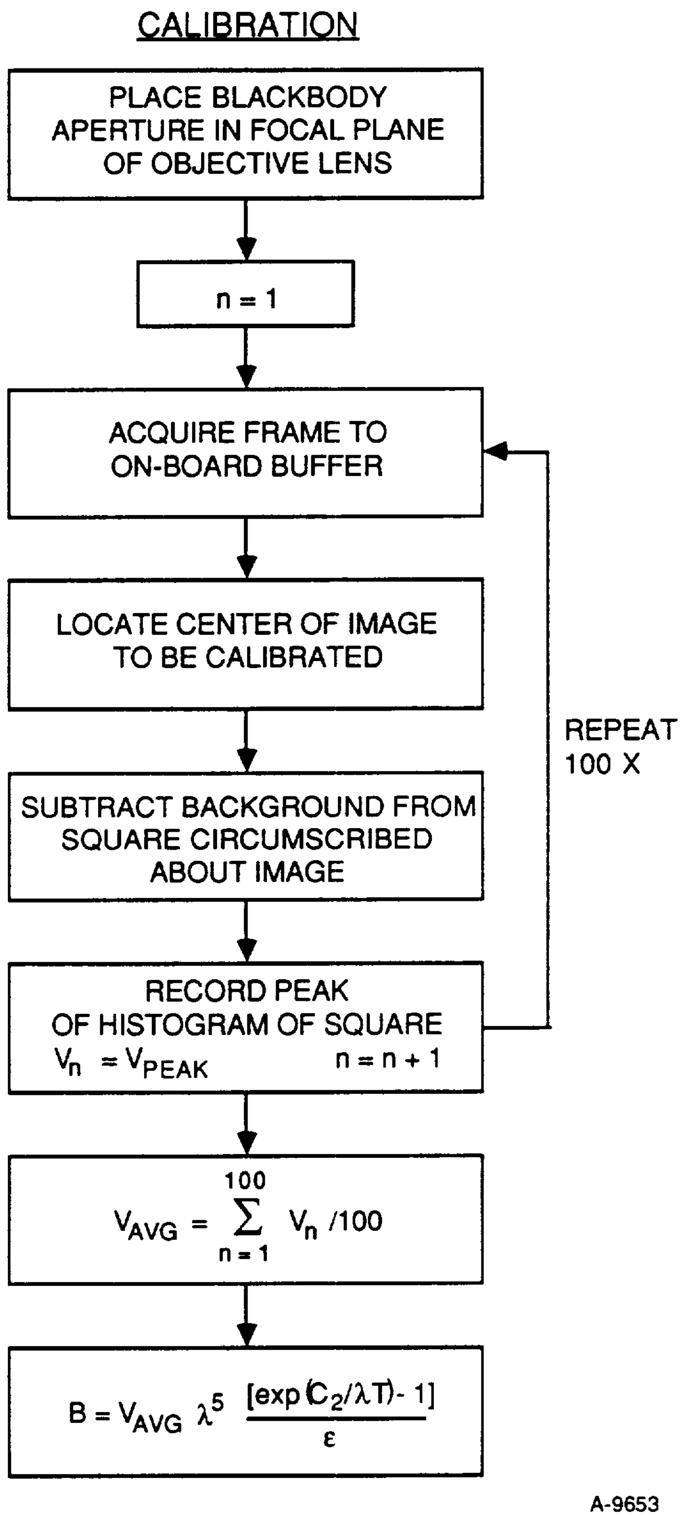

Figure 16. Flowchart of calibration procedure.

4.4 Temperature Measurement

The temperature measurement procedure combines all of the steps described above, as shown in the flowchart of Figure 17. A frame containing up to six images of the hot moving object is acquired and stored in a frame buffer. The appropriate one of the six images is located and the background subtracted from a square area surrounding that image. The result is passed through an output lookup table and displayed on the video monitor as a false color image corresponding to the temperature distribution in the object. This lookup table may be the same one as was created during the calibration procedure, or may be modified to account for any user knowledge of the object's emissivity. In addition to displaying a temperature map, the algorithm finds the mode of the temperature distribution within the object and displays this value in numerical form. This value may also be used in a feedback loop to actively control the temperature.

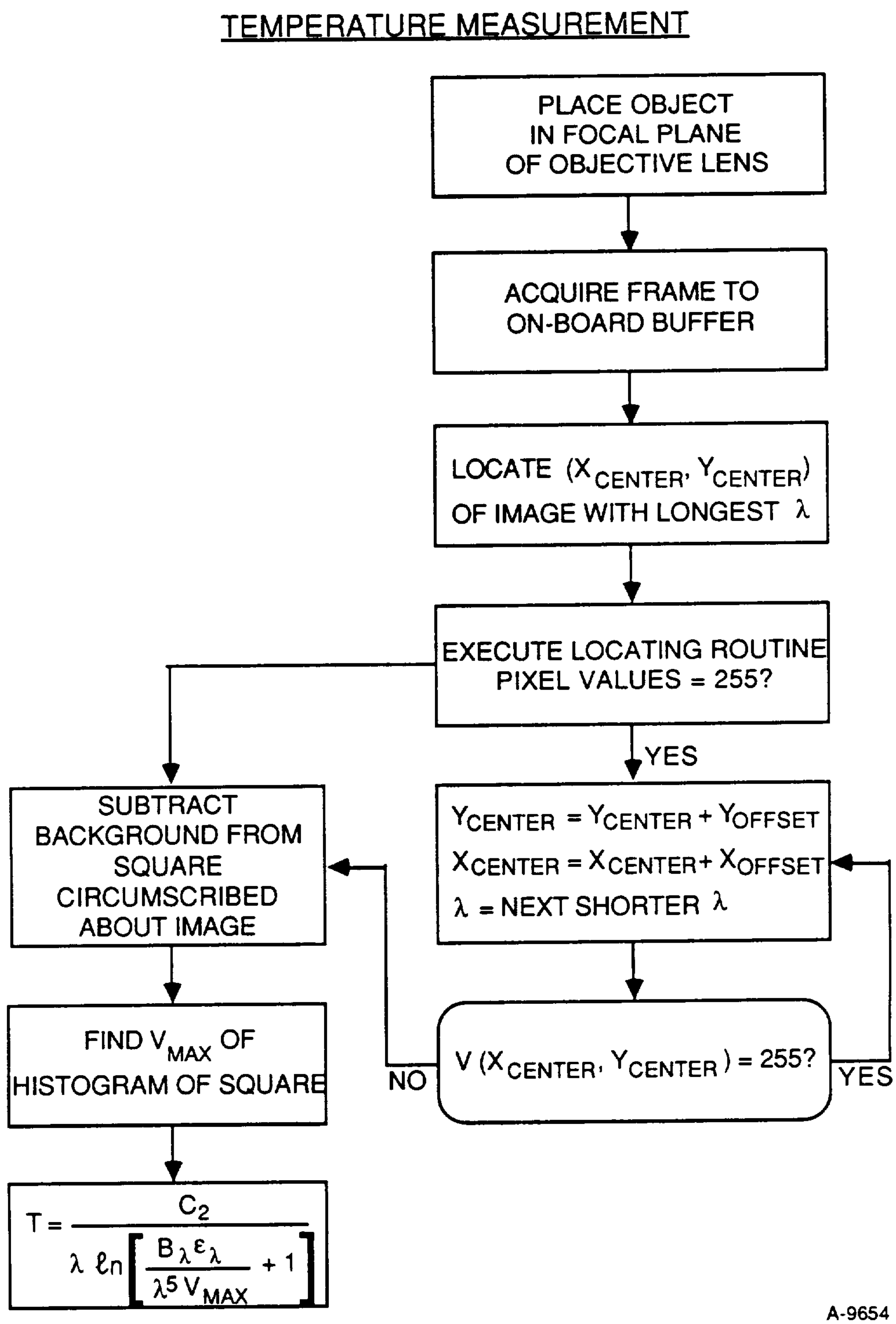

Figure 17. Flowchart of temperature measurement procedure.

5. FUTURE ACTIVITIES

In the upcoming quarter we plan to assemble a complete six-color pyrometer according to the plans described above. Concurrently, the breadboard device will be used to study temperature measurement procedures under difficult conditions similar to those expected to be encountered during acoustic levitation experiments. In particular, we intend to demonstrate the feasibility of accurately measuring temperatures of liquid metals contained in clear quartz crucibles and heated within a kiln having a small viewport. These experiments will suffer many of the difficulties, such as low emissivity specular surfaces and background radiation, expected to be encountered during materials processing in space.

REFERENCES

1. Allen, M. and Frish, M., Multicolor Pyrometer for Materials Processing in Space - Phase II, PSI TR-731, Quarterly Report No. 1, November 1987.

2. Frish, M. and Frank, J., Multicolor Pyrometer for Materials Processing in Space - Phase II, PSI TR-764, Quarterly Report No. 2, February 1988.

3. Frish, M. and Frank, J., Multicolor Pyrometer for Materials Processing in Space - Phase II, PSI TR-796, Quarterly Report No. 3, May 1988.

4. Frish, M., Frank, J., and Beerman, H., Multicolor Pyrometer for Materials Processing in Space - Phase II, PSI TR-862, Quarterly Report No. 4, August 1988.